Design and Hydrodynamic Characterization of a Draft Tube Baffle Tank for Lab-Scale

Mira Schmalenberg*, Anna-Katharina Nocon, and Norbert Kockmann

DOI: 10.1002/cite.201900078

Supporting Information available online

For process development on lab-scale, it is necessary to have equipment that represents the industrial apparatuses as similar as possible to offer short time-to-market. Accordingly, a draft tube baffle (DTB) crystallizer was scaled down from typical m^3-scale to 1 L filling volume. The suspension characteristics were determined for fluidized crystals in saturated solution. For further characterization of the DTB tank, the residence time of the liquid and solid phases were experimentally determined for the continuous operation mode. Additionally, the classifying behavior of the particles in the DTB was investigated.

Keywords: Continuous particle classification, Draft tube baffle, Laboratory stirring tank, Miniaturized crystallizer, Suspension behavior

Received: May 24, 2019; *revised:* December 09, 2019; *accepted:* December 16, 2019

1 Introduction

For simplified process development it is beneficial to run the processes in apparatuses that are as similar as possible and in similar operating modes in the lab and on large-scale production [1, 2]. In the research project ENPRO2.0-TeiA [3], four different small-scale continuously operated crystallizers are investigated, characterized, and optimized. Particularly interesting is a commercially available continuous oscillatory baffled crystallizer (COBC) [4]. Further continuously operated crystallizers are based on the coiled flow inverter (CFI) design [5], on a cascade of multistage mixed suspension mixed product removal (MSMPR) crystallizers [6, 7], and on the draft tube baffle (DTB) crystallizer, whose draft, construction method and suspension behavior is presented below.

The DTB crystallizer is a continuous stirred tank crystallizer that has already been known for long time [8, 9] and is frequently used in industry [10]. Although the DTB concept was investigated in many aspects [11, 12] with simulated flow behavior [13–15] from different stirrer types [16], its design has been further optimized and is still of interest for research [17]. Interestingly, a DTB reactor is already known from literature, which investigated that mixing speed and hydraulic retention time are important operating parameters for crystallization and sedimentation [18]. The experimental investigations on suspension behavior in tanks have so far usually only been carried out in stirred tanks [19–21], here the form of the DTB and its influence on suspension behavior is examined.

This contribution presents the hydrodynamic behavior of a miniaturized DTB tank. For this purpose, a DTB known from literature is scaled down from 1100 L [12, 14, 22] to a vessel with 1 L of inner volume. The use of chemicals and resources can, thus, be reduced as DTBs of larger volumes have been investigated so far [13, 16, 23]. The investigations concerning the suspension behavior and residence time of the liquid and solid phase in the DTB is important to predict a possible operating window and serve as a basis to reconstruct the DTB optimally. The investigations on classification show the feasibility of fine-grain removal in small-scale apparatus.

2 Scale-Down Method

For the construction of the miniaturized DTB, the three known scale-up criteria for stirrer tanks are investigated for scale-down. The scale-up criteria are: 1) tests with same model system, 2) linear geometry similarity, and 3) transfer criteria with same volume-specific power input, same stirrer tip speed, same suspension state, or same heat transfer coefficient [20, 24].

Mira Schmalenberg, Anna-Katharina Nocon, Prof. Dr.-Ing. Norbert Kockmann
mira.schmalenberg@tu-dortmund.de
TU Dortmund University, Laboratory of Equipment Design, Emil-Figge-Straße 68, 44227 Dortmund, Germany.

Regarding to the first criterion, no specific substance system is set as target system because the crystallizer will be used for general process development. Hence, two different substance systems with different density differences (Sect. 3) are selected for the suspension tests.

The methodology of classical geometric similarity is taken for the scale-down of corresponding lengths, such as diameter d, height H, and draft tube diameter d_{dt} [24]. The model DTB (mod) (Fig. 1, left) is known from literature [12, 14, 22], which has a capacity of 1100 L. This DTB was sized down to a glass DTB (Fig. 1, right) with a capacity of 1.2 L.

In a first step, the dimensions were reduced by a factor of 10, although this was not possible for every length, as there are standardized sizes in glass apparatus construction. Therefore, the reduction factor μ (Eq. (1)) is 10–12.5 depending on the corresponding length.

$$\mu = \frac{d_{mod}}{d} = \frac{H_{mod}}{H} = \ldots \approx 10 - 12.5 \quad (1)$$

In this work, two types of stirrers are considered, propeller and blade stirrer, each with three blades as common for crystallization applications [25, 26]. If an ideal ratio of stirrer diameter d_R to draft tube diameter is to be achieved, which is $d_R/d_{dt} > 0.89$ [27], a distance of 2 mm between draft tube and stirrer is required. Smallest deviations of the construction or the alignment can lead to blocking or destruction of the stirrer. To reduce this risk, both stirrers have a diameter of 33 mm and, thus, only a ratio of $d_R/d_{dt} = 0.83$. Both stirrer blades have an inclination of about 45° and were fabricated of glass. In the following, only the results of the blade stirrer are presented, since the required speeds for complete suspension were higher with the propeller stirrer than with the blade stirrer.

Since the stirrer power cannot be determined for lab-scale easily [28], the transfer criterion for same specific power input was not applied. Suspension state and stirrer tip speed were determined as transfer criterion, while heat transfer is not subject of this contribution.

3 Experimental Methods

The experimental setup used for the present investigation is shown in Fig. 2. Used devices are listed in the Supporting Information (SI, Tab. S1). The tracer substance or suspension is provided from the storage vessel. The liquid is then pumped into the lower inlet of the DTB via a peristaltic pump in a Tygon® XL–60 tube (d_i = 1/8', d_o = 1/4', Saint-Gobain Performance Plastics, France). The 3-pitched-blade impeller is driven by an agitator, where the impeller shaft is sealed in the DTB by a grinded glass connection. The DTB as well as the impeller were manufactured by the university's own glassblower workshop. The medium is transported by a peristaltic pump, too. Depending on the type of experiment, the medium is transported through the UV detector or directly into the collection vessel, which is located on a scale. The peristaltic pump (2) with Tygon® S3 E–3603 tube (d_i = 1/8', d_o = 1/4', Saint-Gobain Performance Plastics, France) is used for tests carried out with the fine grain removal system. The entire system was operated at ambient conditions.

3.1 Residence Time Distribution

The residence time distribution of single-phase flow (RTD_L) represented by deionized water is determined from a step signal. Based on the method of Kurt et al. [29] a sodium

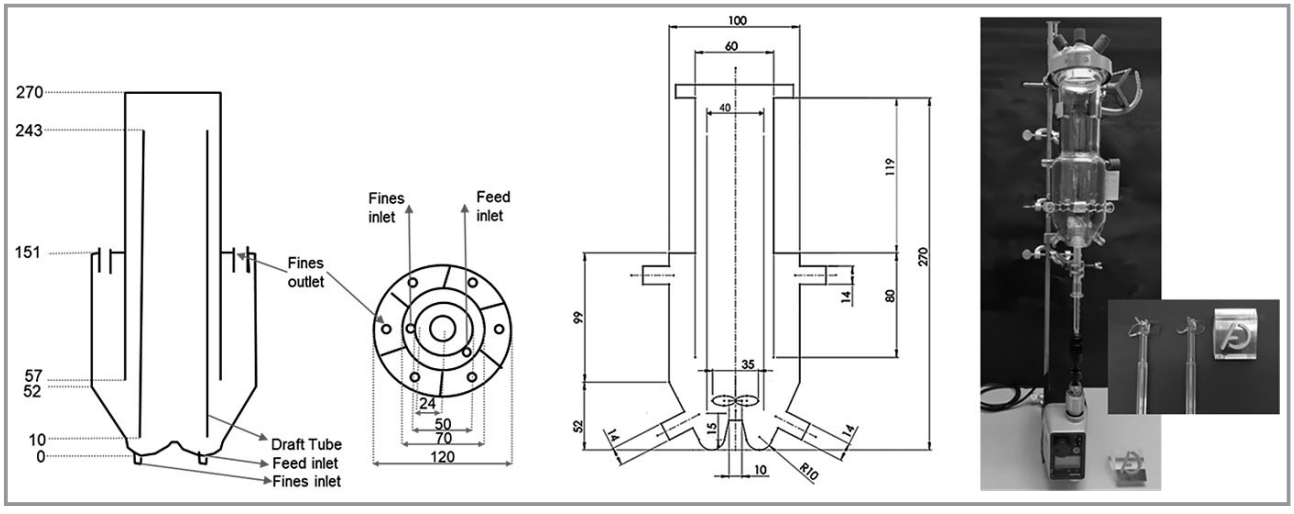

Figure 1. Left: model DTB geometry side view and top view (left) [14], dimensions in cm. Middle: down-scaled DTB geometry side view, dimensions in mm. Right: miniaturized glass DTB.

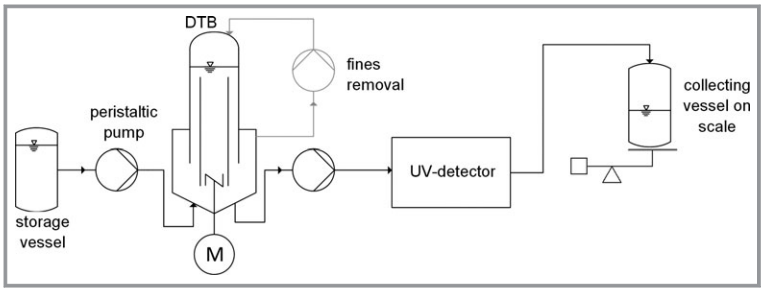

Figure 2. Schematic test setup for the different experiments.

thiosulfate (Panreac, 99.0 %, Germany) tracer is used and detected in a flow-through cuvette in the UV detector. The process mass flow rate is 15.4 ± 0.2 g min^{-1} (2.57 · 10^{-4} kg s^{-1}), mass flow rate of the fines removal is 4.4 ± 0.5 g min^{-1} (7.33 · 10^{-5} kg s^{-1}), and the stirrer speed is set to 380 min^{-1}.

The RTD$_S$ behavior of the solid phase in the DTB is also measured from a step signal. In preparation of the RTD$_S$ measurement, the DTB is filled with saturated acetylsalicylic acid (ASA)-water solution. The storage vessel contains the prepared suspension for the step signal, stirred by a magnet stirrer on a stirrer plate. Therefore, a defined suspension is prepared with saturated ASA (99.0 %, ARCOS Organics, France) in water, based on the data of Apelblat and Manzurola [30] and defined sieved ASA crystals as tracer particles. Two different fractions of sieved crystals were used: a finer grain with 90–180 µm and larger crystals with 250–400 µm. Additionally, the particle size distribution (PSD) of the sieved fractions were measured by a sedimentation method in a spectrometer as described in [31]. The particle weight fraction of the suspension was 0.01 g g$_{sus}^{-1}$.

The concentration of the solid phase is determined by gravimetric measuring method similar to Hohmann et al. [31], which is also used for the determination of the step signal at the outlet of the DTB and is explained in detail in the SI (Sect. S1). The stirrer speed is set to 380 min^{-1} during the investigations, before the step signal is started with a mass flow rate of 15.3 ± 0.1 g min^{-1}(2.55 · 10^{-4} kg s^{-1}).

3.2 Suspension Behavior

To determine the suspension behavior in the DTB two different substance test systems are investigated. Glass spheres (behr Labor-Technik GmbH, 6304531 and 6201225, Germany) of different sizes represent round particles with a density difference to water of $\Delta\rho \approx 1233\,\mathrm{kg\,m^{-3}}$. The other test system is the same as for the determination of RTD$_S$ with additional size and weight fractions. The density difference in water is $\Delta\rho \approx 353\,\mathrm{kg\,m^{-3}}$. The investigated size and weight fractions of the two test systems are listed in the SI (Tab. S2).

The stirrer tip speed u_{tip} can be determined for each measurement according to Eq. (2) with the use of the stirrer diameter d_R and rotation speed n.

$$u_{tip} = \pi n d_R \tag{2}$$

However, in order to determine the suspension status, the measurement procedure must be defined beforehand. The most common criterion is the layer height, where a homogeneous suspension is assumed if the suspended particle layer is 90 % of the liquid height and a particle-free liquid layer can still be seen [19]. The 1-second criterion is often used to describe complete suspension, where the particles on the bottom of the vessel are resuspended within 1 s [32]. These two criteria could not properly be observed in the case of the miniaturized DTB, so that a rather rarely used criterion of "100 % suspension" was chosen [33]. Here, no particle should settle on the bottom of the vessel. Therefore, a suspension is prepared as described in Sect. 3.1 and filled in the closed DTB as shown in Fig. 3.

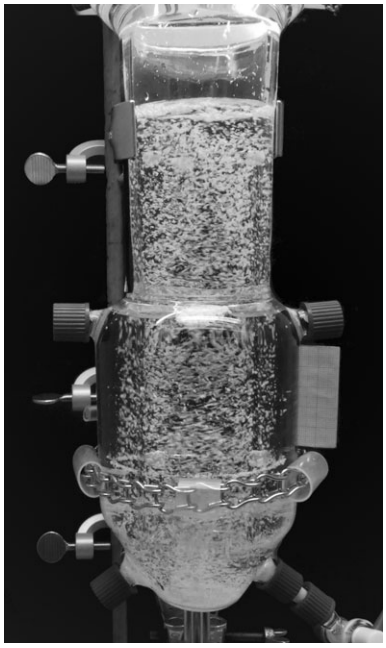

Figure 3. Miniaturized DTB during suspension behavior investigations; filled with 1 L suspension and a solid weight fraction of 0.01 ASA particles of 250–400 µm.

The stirrer speed was gradually increased until the desired circulation flow is achieved, and no particles remain on the bottom. A triple determination was carried out, which was divided into a coarse and two precise determinations, which is described in detail in the SI (Sect. S2).

3.3 Particle Classification Behavior

A suspension was prepared for the investigations of the classification behavior with a solid factor of 0.01 g g$_{sus}^{-1}$

ASA particles in saturated water solution. The solid fraction consisted of four different sieved particle size fractions, which simulate different crystal sizes in the DTB. The exact ASA mass for each fraction is given in Tab. 1.

Table 1. Mass of ASA particles in 1.101 kg suspension for classification behavior investigations.

x_p [µm]	m_{ASA} [g]
< 90	1.003
90–180	2.010
180–250	2.998
250–400	5.001

To simulate a continuous mode, the prepared suspension was pumped in a loop (15.26 ± 0.4 g min^{-1}) during the entire experiment (inlet is equal to outlet). In addition, the peristaltic pump (2) removing suspension from the upper connection and pumping back into the top lid of the DTB (5.8 ± 0.6 g min^{-1}) simulated fine grain removal. This enabled sampling from the main feed stream and the fine grain loop. These suspension samples are taken three times and measured by the sedimentation method (as described in Sect. 3.2) to compare the PSD of these streams. The tests were carried out at four different stirrer speeds (300 min^{-1}, 400 min^{-1}, 500 min^{-1}, and 600 min^{-1}).

4 Results

A hydrodynamic characterization of the constructed DTB follows and should serve as a basis to construct a revised and temperature-controlled DTB.

4.1 Residence Time Distribution

Using the step signal and the change of the concentration or the solid fraction over the time, the residence time sum function $F(t)$ is determined according to Eq. (3), where the tracer composition (c_0, w_0) must be known [34].

$$F(t) = \frac{c(t)}{c_{0,\text{tracer}}} \quad \text{or} \quad F(t) = \frac{w(t)}{w_{0,\text{tracer}}} \tag{3}$$

The model for ideal stirring vessels according to Eq. (4) describes the residence time behavior of the DTB, which belongs to the continuous stirring vessels. The fluid dynamic residence time τ is determined by the ratio of volume-to-volume flow rate (Eq. (5)) and the actual mean residence time $\bar{t}$ by Eq. (6). [34]

$$F(t) = 1 - \exp\left(-\frac{t}{\tau}\right) \tag{4}$$

$$\tau = \frac{V}{\dot{V}} \tag{5}$$

$$\bar{t} = \int_0^1 t\,\mathrm{d}F(t) = \int_0^\infty (1 - F)\,\mathrm{d}t \tag{6}$$

The calculated fluid dynamic and actual residence times for the respective tests of the different phases and adjusted mass flow rates used for the determination of the residence time are listed in Tab. 2 for the investigated suspensions.

Table 2. Residence times for three different phases and their mass flow rates.

Phase	$\dot{m}_{process}$ [g min^{-1}]	$\dot{m}_{fines}$ [g min^{-1}]	τ [min]	$\bar{t}$ [min]
Single fluid phase, RTD_L	15.4 ± 0.2	4.4 ± 0.5	66.4	63.7
Solid phase (90 -180 µm), RTD_{S1}	15.3 ± 0.1	–	67.0	55.8
Solid phase (250–400 µm), RTD_{S2}	15.3 ± 0.1	–	66.9	46.3

Fig. 4 shows the results of the RTD investigations as function of time. As expected, the investigated phases exhibit a residence time behavior corresponding to a stirred tank. The RTD_L (squares ■) corresponds directly to the behavior of a continuously operated stirred tank (CSTR) (line). Additionally, the hydrodynamic and actual residence times are almost the same. This is an indicator that there is no dead volume for the liquid phase. The RTD_S of the solid phase (circle ● and diamond◆) show a slightly different relationship to the ideal CSTR RTD_L. The shorter actual residence time in Tab. 2 also confirms this behavior. The particles stay shorter in the DTB than the liquid phase. Due to the higher solid density of the particle, they sink to the bottom. Thus, the probability of the particles staying at the crystallizer bottom increases compared to the single fluid element [24], leading to the shorter residence time. This indicates that the particle residence time could be influenced by the stirrer speed. Additionally, the results show that the smaller particles remain in the DTB for a longer time (about 10 min) than the larger ones.

This behavior is desired for the operation of the DTB, as smaller particles should stay longer in order to grow further. However, the presented investigations are not crystallization experiments, so that no exact statement is possible on the influence of residence time during crystallization.

4.2 Suspension Behavior

The determination of the suspension behavior should be the base for determining the operating window of the DTB.

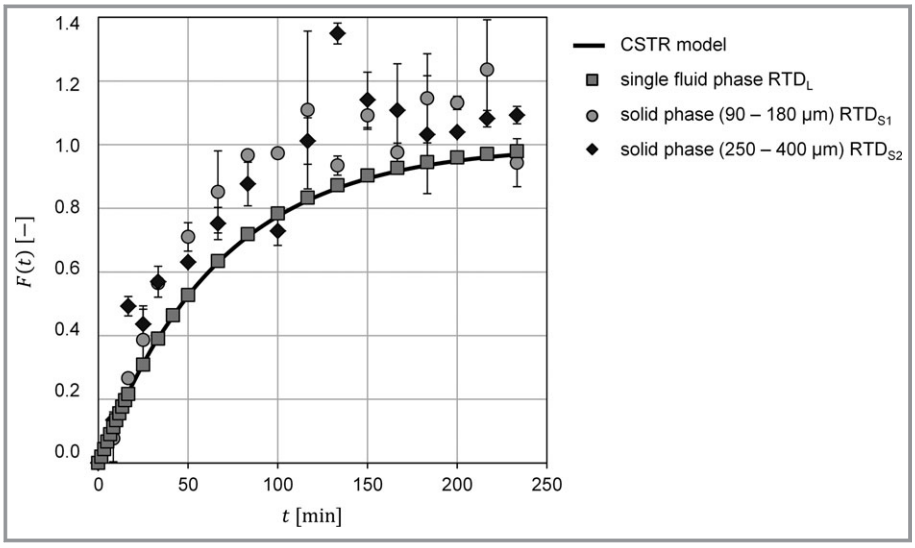

Figure 4. Residence time distribution for three different phases as function of the time.

As already mentioned, the stirrer tip speed is a scale-up criterion that is easy to determine during suspension investigations. It can be calculated according to Eq. (2). Fig. 5 shows the results of the suspension investigations. The stirrer tip speed required for complete suspension is plotted for different particle sizes and systems as a function of the volume fraction of solids φ, which describes the volume ratio of solid ASA or glass V_S and suspension volume V_{sus} (Eq. (7)).

$$\varphi = \frac{V_S}{V_{sus}} \tag{7}$$

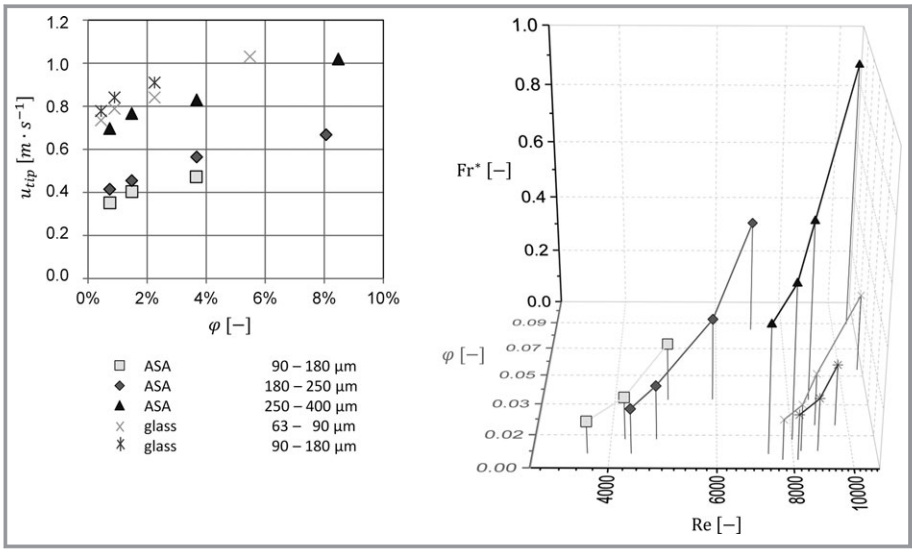

Figure 5. a) Required stirrer tip speed for complete suspension as a function of solid volume fraction for different particle sizes and substance systems; b) 3D illustration of the same results as in Fig. 5a in dependency of Froude and Reynolds number.

As expected, the results show that higher stirrer speed is required to ensure complete suspension as particle size or the solids volume fraction of a substance system increases. Additionally, the density difference of the substance system strongly influences the suspension. These results indicate that the relatively small glass particles in water (63–180 µm) need similar stirrer tip speeds as larger ASA particles (250–400 µm). The maximum possible stirrer tip speed with the glass grinded sealing of the stirrer shaft is limited to 1.037 m s^{-1}, hence, the operating window is sufficiently investigated with the selected substance systems. This is the reason why no higher suspension densities can be realized in this DTB design to suspend, although the DTB in common is known for handling high suspension densities. This observation leads to the conclusion that stirrer systems from below are not beneficial for small-scale tanks due to the leakage problem.

If the suspension behavior is to be regarded as the transfer criterion, the Reynolds and Froude numbers are relevant as key figures. The stirrer Reynolds number *Re* (Eq. (8)) is used to describe the flow situation and the Froude number *Fr** (Eq. (9)) relates the centrifugal acceleration to gravitational acceleration. [24, 28]

$$Re = \frac{n d_R^2 \rho_L}{\eta_L} \tag{8}$$

$$Fr^* = \frac{n^2 d_R \rho_L}{g(\rho_S - \rho_L)} \tag{9}$$

The same results from Fig. 5a are illustrated in Fig. 5b in the 3-dimensional diagram, where the *x*-axis represents the stirrer Reynolds number, the *y*-axis the solid volume fraction and the *z*-axis the Froude number. In this application, it is obvious that higher Reynolds numbers are necessary with higher solids content in order to ensure complete suspension. Since the rotational speed is also included in the Froude number, it is also higher with higher solids content and increasing particle size for complete suspension. Based on these

investigations, the operating window for suspending in the DTB is determined.

4.3 Particle Classification Behavior

The samples taken at the process outlet and fine grain discharge should provide information on the classification quality the DTB is designed for. The PSD of the samples are measured with the described sedimentation method and the mean particle diameter ($x_{50,3}$) is determined. Each PSD measurement is done at least three times and the results of these experiments are given in Tab. 3.

Table 3. Particle mean diameter in process and fine flow for different stirrer speeds.

n [min^{-1}]	$x_{50,3}$ process samples [µm]	$x_{50,3}$ fine grain samples [µm]
300	190 ± 16	57 ± 5
400	199 ± 8	46 ± 5
500	184 ± 12	63 ± 8
600	192 ± 23	82 ± 20

According to the results, the average particle diameter of the process stream is significantly larger than that of the fine-grain removal. This means that the crystals used are already classified at the lower stirrer speeds. The samples at the fine grain removal show significantly smaller particle diameters between 40–100 µm. In addition, a dependence on the average particle diameter as a function of the stirrer speed is evident. The higher the stirrer speed, the larger is the mean particle diameter in the fine grain loop. These results show that classification in the miniaturized DTB is possible and that the particle size in the fine grain discharge can be controlled with the aid of the stirrer speed.

5 Summary and Outlook

This contribution presents a draft tube baffle (DTB) tank known from literature, which is scaled down from 1100 L pilot size to a 1-L laboratory glass apparatus by means of geometric similarity. Hydrodynamic investigations were made in the DTB tank including the determination of the residence time behavior of the liquid and solid phase, which can be described by the RTD of a CSTR. In addition, the suspension behavior in the DTB has been investigated in order to determine the DTB operating window. Investigations of the classification behavior show that classification in the miniaturized DTB is possible and can be influenced by the stirrer speed. In the future, the DTB will be further developed enable heating and cooling of the device for crystallization experiments.

The German Federal Ministry for Economic Affairs and Energy (BMWi) is acknowledged for funding this research as part of the ENPRO2.0 initiative (Ref. no. 03ET1528A). We acknowledge financial support by TU Dortmund University within the funding programme Open Access Publishing. The authors would like to thank our technician Carsten Schrömges and the workshop of the TU Dortmund for glassblowing results without such research would not have been possible.

Symbols used

c_w	[–]	resistance coefficient
d	[m]	diameter
$F(t)$	[–]	residence time sum function
Fr^*	[–]	Froude number
g	[m s^{-2}]	acceleration of gravity
H	[m]	height
$\dot{m}$	[kg s^{-1}]	mass flow rate
n	[s^{-1}]	rotation speed
Re	[–]	stirrer Reynolds number
Re_p	[–]	particle Reynolds number
t	[s]	time
$\bar{t}$	[s]	actual mean residence time
u_{tip}	[m s^{-1}]	stirrer tip speed
V	[m^3]	volume
$\dot{V}$	[m^{3}L^{-1}]	volume flow rate
w	[g g^{-1}]	weight fraction
$x_{50,3}$	[µm]	mean particle diameter

Greek letters

η	[Pa s]	dynamic viscosity
μ	[–]	scaling factor
ρ	[kg m^{-3}]	density
τ	[s]	fluid dynamic residence time
φ	[–]	volume fraction of solid

Sub- and Superscripts

dt	draft tube
i	inside
L	liquid phase
mod	model
o	outside
P	particle
R	stirrer
S	solid phase
sus	suspension
0	start

Abbreviations

ASA	acetylsalicylic acid
CFI	coiled flow inverter
COBC	continuous oscillatory baffled crystallizer
DTB	draft tube baffle
MSMPR	multistage mixed suspension mixed product removal
PSD	particle size distribution
RTD_L	residence time distribution liquid phase
RTD_S	residence time distribution solid phase

References

[1] S. Lier, J. Riese, G. Cvetanoska, A. K. Lesniak, S. Müller, S. Paul, L. Sengen, M. Grünewald, *Chem. Eng. Process.* **2018**, *123*, 111–125. DOI: https://doi.org/10.1016/j.cep.2017.10.026

[2] T. Bieringer, S. Buchholz, N. Kockmann, *Chem. Eng. Technol.* **2013**, *36 (6)*, 900–910. DOI: https://doi.org/10.1002/ceat.201200631

[3] www.enpro-initiative.de (Accessed on May 15, 2019)

[4] www.nitechsolutions.co.uk (Accessed on May 07, 2019)

[5] M. Schmalenberg, L. Hohmann, N. Kockmann, Miniaturized Tubular Cooling Crystallizer With Solid-Liquid Flow for Process Development, in *ASME 2018 16th ICNMM* 2018, Paper No. V001T02A006, Dubrovnik **2018**. DOI: https://doi.org/10.1115/ICNMM2018-7660

[6] M.-C. Lührmann, J. Timmermann, G. Schembecker, K. Wohlgemuth, *Cryst. Growth Des.* **2018**, *18 (12)*, 7323–7334. DOI: https://doi.org/10.1021/acs.cgd.8b00941

[7] M.-C. Lührmann, M. Termühlen, J. Timmermann, G. Schembecker, K. Wohlgemuth, *Chem. Eng. Sci.* **2018**, *192*, 840–849. DOI: https://doi.org/10.1016/j.ces.2018.08.007

[8] H. B. Caldwell, *Ind. Eng. Chem.* **1961**, *53*, 115–118. DOI: https://doi.org/10.1021/ie50614a023

[9] J. W. Mullin, *Crystallization*, Butterworths, London **1961**.

[10] W. Beckmann, *Crystallization: Basic Concepts and Industrial Applications*, Wiley-VCH, Weinheim **2013**.

[11] R. A. Eeek, S. Dijkstra, G. M. Rosmalen, *AIChE J.* **1995**, *41*, 571–584. DOI: https://doi.org/10.1002/aic.690410315

[12] A. M. Neumann, *Characterizing industrial crystallizers of different scale and type*, Doctoral thesis, TU Delft **2001**.

[13] W. Wantha, A. E. Flood, *Chem. Eng. Commun.* **2008**, *195 (11)*, 1345–1370. DOI: https://doi.org/10.1080/00986440801963527

[14] A. ten Cate, S. K. Bermingham, J. J. Derksen, H. M. J. Kramer, in *10th European Conf. on Mixing* (Eds: H. E. A. van den Akker, J. J. Derksen), Elsevier, Delft **2000**, 255–264.

[15] H. Pan, J. Li, Y. Jin, B. Yang, X. Li, *Int. J. Chem. Eng.* **2016**, *2016 (5)*, 1–11. DOI: https://doi.org/10.1155/2016/6862152

[16] H. J. Pant, *Appl. Radiat. Isot.* **2000**, *53 (6)*, 999–1004. DOI: https://doi.org/10.1016/S0969-8043(99)00256-0

[17] X. Song, M. Zhang, J. Wang, P. Li, J. Yu, *Ind. Eng. Chem. Res.* **2010**, *49 (21)*, 10297–10302. DOI: https://doi.org/10.1021/ie100786f

[18] K. Xu, C. Wang, X. Wang, Y. Qian, *Chemosphere* **2012**, *88 (2)*, 219–223. DOI: https://doi.org/10.1016/j.chemosphere.2012.02.061

[19] W.-D. Einenkel, A. Mersmann, *Verfahrenstechnik (Mainz)Verfahrenstechnik; vt, Mainz* **1977**, *11 (2)*, 90–94.

[20] M. W. Chudacek, *Ind. Eng. Chem. Fundam.* **1986**, *25*, 391–401. DOI: https://doi.org/10.1021/i100023a015

[21] M. Kraume, P. Zehner, *Chem. Ing. Tech.* **1988**, *60 (11)*, 822–829. DOI: https://doi.org/10.1002/cite.330601104

[22] S. K. Bermingham, A. M. Neumann, P. J. T. Verheijen, H. J. M. Kramer, in *14th Int. Symp. on Industrial Crystallization*, Institution of Chemical Engineers, Rugby **1999**.

[23] D.-H. Oh, R.-Y. Jeon, J.-H. Kim, C.-H. Lee, M. Oh, K.-J. Kim, *Cryst. Growth Des.* **2019**, *19 (2)*, 658–671. DOI: https://doi.org/10.1021/acs.cgd.8b01237

[24] M. Stiess, *Mechanische Verfahrenstechnik – Partikeltechnologie 1*, 3rd ed., Springer, Berlin **2009**.

[25] M. Neumann, S. K. Bermingham, H. J. M. Kramer, G. M. van Rosmalen, *J. Cryst. Growth* **1999**, *198*, 723–728. DOI: https://doi.org/10.1016/S0022-0248(98)01193-2

[26] C. V. Rane, K. Ekambara, J. B. Joshi, D. Ramkrishna, *AIChE J.* **2014**, *60 (10)*, 3596–3613. DOI: https://doi.org/10.1002/aic.14541

[27] G. M. Westhoff, H. J. M. Kramer, P. J. Jansens, J. Grievink, *Chem. Eng. Res. Des.* **2004**, *82 (7)*, 865–880. DOI: https://doi.org/10.1205/0263876041596670

[28] M. Kraume, *Mischen und Rühren*, Wiley-VCH, Weinheim **2003**.

[29] S. K. Kurt, M. G. Gelhausen, N. Kockmann, *Chem. Eng. Technol.* **2015**, *38 (7)*, 1122–1130. DOI: https://doi.org/10.1002/ceat.201400515

[30] A. Apelblat, E. Manzurola, *J. Chem. Themodyn.* **1999**, *31*, 85–91.

[31] L. Hohmann, M. Schmalenberg, M. Prasanna, M. Matuschek, N. Kockmann, *Chem. Eng. Technol.* **2019**, *360*, 1371–1389. DOI: https://doi.org/10.1016/j.cej.2018.10.166

[32] T. N. Zwietering, *Chem. Eng. Sci.* **1958**, *8 (3–4)*, 244–253. DOI: https://doi.org/10.1016/0009-2509(58)85031-9

[33] G. Staudinger, F. Moser, *Chem. Ing. Tech.* **1976**, *48 (11)*, 1071. DOI: https://doi.org/10.1002/cite.330481128

[34] G. Emig, E. Klemm, *Chemische Reaktionstechnik*, Springer, Berlin **2017**.

